

Role of Quorum Sensing in Chlorine Tolerance and Enhancement of Chlorination Efficiency via Quorum Quenching

Yuhao Xie, Shiyu Lv, Junyan Chen, Zedong Lu*

College of Architecture and Civil Engineering, Beijing University of Technology, Beijing, 100124, China

**Corresponding Author*

Keywords: Free Chlorine Disinfection; Quorum Sensing; Quorum Quenching; Extracellular Polymeric Substances; Chlorine Tolerance

Abstract: Chlorine disinfection is the most widely used method for microbial control in water treatment; however, some bacteria can survive chlorine exposure and develop chlorine tolerance, the underlying mechanisms of which remain unclear. In this study, *Escherichia coli*, *Pseudomonas aeruginosa* PAO1, and *Acinetobacter* CR26 were selected as model strains to systematically investigate the role of quorum sensing (QS) in chlorine tolerance and to evaluate the potential of quorum quenching (QQ) in enhancing chlorination efficiency. Under 0.5 mg/L free chlorine, the total AHLs in the three strains decreased by 40.8%, 61.1%, and 43.8% within 1.5 min, respectively. However, the chlorine-tolerant strains PAO1 and CR26 exhibited pronounced signal recovery or maintenance, whereas *E. coli* showed a weak response. Correlation analysis identified C8, C6, and C12-HSL as the dominant signal molecules most closely associated with extracellular polymeric substances (EPS) in the three strains, respectively. Inactivation results revealed that chlorine tolerance followed the order of CR26 > PAO1 > *E. coli*, with maximum log reductions of 1.79, 3.09, and 3.22 at 20 min, respectively. Furthermore, QQ significantly suppressed EPS production and mitigated residual chlorine decay in chlorine-tolerant bacteria. For instance, in CR26, AT500 reduced chlorine decay by approximately 50% at 30 min, while SAH500 decreased EPS from 4.0 to 3.05 mg/L at 20 min and enhanced inactivation efficiency by about 23%. Overall, QS contributes to bacterial chlorine tolerance by regulating EPS-associated extracellular defense, whereas QQ can effectively disrupt this protection and enhance chlorination performance, highlighting its potential as a strategy for controlling chlorine-tolerant bacteria.

1. Introduction

Chlorine disinfection has been widely applied in drinking water treatment and other water systems due to its high efficiency, low cost, and ability to maintain residual disinfectant (He et al., 2023; Wang et al., 2025)[11,28]. However, increasing evidence indicates that certain bacteria can survive chlorination and exhibit varying degrees of chlorine tolerance, posing potential risks to water quality and public health (Zhu et al., 2020; Gupta et al., 2022; Jathar et al., 2021)[4,9,14]. Bacterial chlorine

tolerance is generally considered to be a multifactorial phenomenon associated with various physiological and phenotypic responses (Jathar et al., 2023; Xue et al., 2013) [13,31]. Among these, extracellular polymeric substances (EPS) have been recognized as a key protective component (Flemming et al., 2025; Harimawan and Ting, 2016; Seviour et al., 2019) [6,10,25]. EPS can not only react with and consume disinfectants but also act as a physical barrier that limits the penetration of oxidants to cell surfaces, thereby reducing disinfection efficiency (Flemming et al., 2023; Lv et al., 2024) [7,17].

Quorum sensing (QS) is a cell–cell communication mechanism mediated by small signaling molecules, typically N-acyl homoserine lactones (AHLs) in Gram-negative bacteria (Miller and Bassler, 2001; Papenfort and Bassler, 2016; Waters and Bassler, 2005) [21,23,29]. QS regulates a wide range of collective behaviors related to environmental adaptation, including biofilm formation, secretion of extracellular products, stress response, and virulence expression (Davies et al., 1998a, 1998b; Parsek and Greenberg, 2005) [3,24]. Previous studies have suggested that QS plays an important role in regulating EPS production, implying that it may contribute to bacterial tolerance to environmental stresses (McLean et al., 2006) [19]. In chlorination systems, QS may therefore participate in chlorine tolerance by modulating EPS-associated defense responses. However, the role of QS under chlorination conditions remains insufficiently understood. In particular, the dynamic behavior of AHLs under chlorine stress, their quantitative relationship with EPS production, and their potential linkage to bacterial inactivation processes have not been systematically elucidated, especially for planktonic bacteria (Borchardt et al., 2001; Keltsch et al., 2025; Michels et al., 2000) [1,15,20].

In addition to mechanistic understanding, targeting QS also provides a potential strategy for enhancing chlorination efficiency. Quorum quenching (QQ), which disrupts QS through inhibition of signal synthesis, degradation of signaling molecules, or interference with signal perception, has been widely reported to suppress biofilm formation and reduce bacterial virulence (Chen et al., 2013; Dong et al., 2001; Hentzer, 2003) [2,5,12]. Nevertheless, whether QQ can enhance chlorine disinfection by interfering with QS-regulated EPS production and extracellular defense processes remains unclear. Moreover, the responses of bacteria with different levels of chlorine tolerance to QQ have not been fully investigated (Fu et al., 2025; Sohail and Martienssen, 2026) [8,26].

In this study, *Pseudomonas aeruginosa* PAO1 and *Acinetobacter* CR26, representing chlorine-tolerant bacteria, and *Escherichia coli* as a chlorine-sensitive reference strain, were selected as model organisms [5]. Under a free chlorine concentration of 0.5 mg/L, the dynamics of AHL signal molecules during chlorination were systematically analyzed, and their relationships with EPS production and bacterial inactivation were evaluated. Furthermore, different quorum quenching agents were introduced to investigate their effects on residual chlorine decay, EPS secretion, and disinfection performance [8]. The aim of this work is to elucidate the role of QS in bacterial chlorine tolerance, clarify the mediating role of EPS between QS signaling and phenotypic resistance, and explore the potential of QQ as a strategy to enhance chlorination efficiency.

2. Materials and methods

2.1 Experimental materials

The bacterial strains used in this study included the chlorine-tolerant *Pseudomonas aeruginosa* PAO1 and *Acinetobacter* CR26, as well as the chlorine-sensitive reference strain *Escherichia coli*. Chlorination experiments were conducted using sodium hypochlorite solution as the disinfectant stock. All chemicals used were of analytical grade and were purchased from Fuchen Chemical Reagent Co., Ltd. (Tianjin, China) [18].

2.2 Experimental setup and operation

Bacterial cultures in the stationary phase were used for all experiments. Prior to chlorination, the cultures were centrifuged three times at 8000 r/min, and the cell pellets were washed with sterile phosphate-buffered saline (PBS) between each centrifugation step. The washed cells were then resuspended in PBS to obtain an initial bacterial concentration of approximately 10^8 CFU/mL.

All experiments were conducted in a 300 mL reaction system with an initial free chlorine concentration of 0.5 mg/L. For the quorum quenching treatments, the quenching agents were added simultaneously with chlorine. Experiments were performed in 500 mL Erlenmeyer flasks equipped with a 1 cm magnetic stir bar and mixed at 300 r/min using a magnetic stirrer[26].

Samples (30 mL) were collected at predetermined time points (0, 1.5, 5, 10, 20min). Immediately after sampling, 100 μ L of 10 g/L sodium thiosulfate solution was added to quench residual chlorine and stop the reaction. The collected samples were subsequently analyzed for EPS, AHL signal molecules, and bacterial biomass[27].

2.3 Data analysis

2.3.1 EPS extraction and measurement method

The bacterial suspension, after removal of the growth medium, was heated in a water bath at 45 °C for 1 h to extract EPS from the cell surface. Under these conditions, cell lysis was minimized while achieving a relatively high EPS extraction efficiency. Subsequently, the suspension was centrifuged at 12,000 r/min for 20 min to remove bacterial cells (excluding EPS), and the supernatant was collected. The organic substances present in the supernatant were considered as EPS. The total EPS content was quantified by measuring the dissolved organic carbon (DOC) concentration of the extracted solution.

2.3.2 Extraction and measurement of AHLs signal molecules

AHLs were extracted and analyzed during the sampling process. Briefly, the bacterial suspension was heated in a water bath, followed by centrifugation at 3000 r/min for 15 min. The supernatant was then filtered through a 0.45 μ m membrane filter (Fisher Scientific, CA, USA). The filtrate was concentrated using solid-phase extraction (SPE) (Fisher Scientific, CA, USA).

The concentrated extract was mixed with an equal volume of acidified ethyl acetate (containing 0.1% acetic acid) and vigorously shaken for 1 h, followed by centrifugation at 3000 r/min for 15 min. The resulting supernatant was further concentrated using HLB SPE cartridges (Millipore Sigma, USA) and evaporated to dryness under a nitrogen stream using a nitrogen evaporator (Organomation, USA).

The dried residue was reconstituted in methanol, spiked with an internal standard at a concentration of 20 ng/mL, and subsequently analyzed using liquid chromatography–tandem mass spectrometry (LC–MS/MS) (Agilent, USA).

2.3.3 Other indicators

The free residual chlorine in water was determined by DPD colorimetry. The biomass of bacteria was counted by plate coating method.

2.4 Statistical analysis

These charts were drawn by Originlab 2021. SPSS statistical software version 26 was used for data analysis. Paired t-test and single sample t-test were performed. The confidence interval was 95%,

and the significant values were <0.05 and 0.01 , respectively. Use Python 3.9 to fit the curve.

3. Results and discussion

3.1 Effect of chlorine disinfection on the content of AHLs

To elucidate the dynamic behavior of quorum sensing (QS) signal molecules during chlorination, the composition and temporal variation of AHLs in *E. coli*, PAO1, and CR26 under free chlorine stress were systematically investigated. Multiple AHLs, including C4-HSL, C6-HSL, 3-oxo-C6-HSL, C8-HSL, C10-HSL, and C12-HSL, were detected in all three bacterial systems, indicating that AHL-mediated QS activity was present in these Gram-negative bacteria under chlorination conditions.

Chlorination markedly disturbed the extracellular AHL pool in all three strains. The data is shown in Figure 1. The initial total AHL concentrations in *E. coli*, PAO1, and CR26 were 0.529, 8.942, and 1.695 $\mu\text{g/L}$, respectively, and decreased to 0.313, 3.482, and 0.952 $\mu\text{g/L}$ at 1.5 min, corresponding to reductions of 40.8%, 61.1%, and 43.8%. These results indicate that free chlorine rapidly disrupts the pre-existing balance of extracellular signaling molecules during the early stage of disinfection, resulting in a sharp depletion of the signal pool. Thereafter, the three strains exhibited distinct recovery patterns, suggesting substantial differences in QS regulatory capacity under chlorine stress.

PAO1 showed the strongest AHL response and the greatest dynamic variation. Six AHLs were detected before chlorination, with a total concentration substantially higher than those in the other two strains. Among them, C4-HSL, C6-HSL, and C12-HSL were the dominant components, with initial concentrations of 3.910, 1.458, and 2.968 $\mu\text{g/L}$, respectively, together accounting for approximately 93.2% of the total AHLs. Upon chlorination, the short-chain signals decreased sharply. At 1.5 min, C4-HSL and C6-HSL dropped to 0.238 and 0.326 $\mu\text{g/L}$, representing decreases of 93.9% and 77.6%, respectively. However, both signals recovered markedly within the following 5 min: C4-HSL increased to 2.044 $\mu\text{g/L}$, corresponding to 52.3% of its initial level, while C6-HSL recovered to 1.026 $\mu\text{g/L}$, or 70.4% of its initial level. At 10 min, C4-HSL still remained at a relatively high level of 2.129 $\mu\text{g/L}$. In contrast, C12-HSL exhibited a gradual declining trend but still maintained a relatively high concentration of 1.733 $\mu\text{g/L}$ at 20 min. These results reveal a typical “initial collapse–subsequent recovery” pattern in PAO1, indicating a strong capacity for QS signal reconstruction under chlorine stress.

In contrast, CR26 displayed a relatively moderate AHL response that was more characteristic of steady-state maintenance. Although six AHLs were also detected in CR26, the initial total concentration was only 1.695 $\mu\text{g/L}$, substantially lower than that of PAO1. C12-HSL was the dominant signal, with an initial concentration of 0.966 $\mu\text{g/L}$, accounting for approximately 57.0% of the total AHLs, followed by C8-HSL (0.309 $\mu\text{g/L}$), C6-HSL (0.170 $\mu\text{g/L}$), and C4-HSL (0.159 $\mu\text{g/L}$). After chlorination, C12-HSL decreased to 0.389 $\mu\text{g/L}$ at 1.5 min, representing a 59.7% reduction, but subsequently recovered to 0.525, 0.430, and 0.622 $\mu\text{g/L}$ at 5, 10, and 20 min, respectively, remaining detectable throughout the experiment. Meanwhile, C6-HSL and C8-HSL fluctuated only slightly and remained within relatively stable low-to-moderate concentration ranges, reaching 0.204 and 0.219 $\mu\text{g/L}$, respectively, at 20 min. Notably, C4-HSL increased to 0.368 $\mu\text{g/L}$ at 10 min, approximately 2.31 times its initial level, suggesting that CR26 may partially regulate stress responses through a local increase in short-chain AHLs while maintaining long-chain dominant signals. Overall, total AHLs in CR26 remained within 1.106–1.269 $\mu\text{g/L}$ during the 5–20 min period, with substantially smaller fluctuations than those observed in PAO1. This indicates that the QS system of CR26 did not undergo extensive reconstruction under chlorine stress, but instead was characterized by sustained dominance of key signals and compensatory local adjustment.

By comparison, *E. coli* exhibited the lowest AHL abundance and the least continuous dynamic response. The initial total AHL concentration was only 0.529 $\mu\text{g/L}$, with C12-HSL as the dominant

signal at 0.339 $\mu\text{g/L}$, accounting for approximately 64.1% of the total. Following chlorination, C12-HSL rapidly decreased to 0.082 $\mu\text{g/L}$ at 1.5 min, a reduction of 75.8%, and further declined to 0.050 $\mu\text{g/L}$ at 5 min. Although it transiently recovered to 0.272 $\mu\text{g/L}$ at 10 min, it became undetectable by 20 min. In parallel, 3-oxo-C6-HSL increased from 0.064 to 0.114 $\mu\text{g/L}$ at 1.5 min, representing a 78.1% increase, but disappeared at 5 min and reappeared at 20 min at 0.106 $\mu\text{g/L}$. C8-HSL showed a similar fluctuation pattern characterized by appearance, disappearance, and reappearance. These findings suggest that although *E. coli* exhibited some degree of AHL response under chlorine stress, its overall signal abundance was low and its dynamic pattern lacked continuity. Unlike PAO1, it did not show clear signal reconstruction, nor did it display the stable maintenance pattern observed in CR26, but rather a weak and discontinuous stress-associated disturbance.

Further comparison of the initial total AHLs clearly showed that PAO1 possessed a much more active QS state prior to chlorination, with total AHL levels approximately 5.28-fold and 16.9-fold higher than those of CR26 and *E. coli*, respectively. When combined with the observed temporal patterns, PAO1 can be characterized by pronounced fluctuations in short-chain signals together with sustained levels of long-chain signals, reflecting a strong capacity for signal-network reconstruction. CR26, by contrast, was characterized primarily by the persistent presence of C12-HSL, indicating a steady-state maintenance response. In *E. coli*, the dominant signals were not sustained during later stages, and the overall pattern lacked regularity, suggesting a relatively weak AHL-mediated communication capacity.

Overall, chlorination not only affected bacterial survival but also substantially perturbed AHL-mediated QS systems. All three strains exhibited an initial decline in total AHLs, indicating that free chlorine first disrupted the pre-existing extracellular signaling pool. During the subsequent phase, PAO1 showed the strongest signal reconstruction capacity, CR26 displayed the greatest signal maintenance capacity, and *E. coli* exhibited only a weak and discontinuous response. These results suggest that chlorine-tolerant bacteria are more likely to maintain or reconstruct AHL-mediated communication networks under chlorine stress, thereby coordinating subsequent collective defense processes.

The observed disturbance of AHLs further suggests that chlorine-tolerant bacteria may preserve or rebuild QS activity under oxidative stress. However, whether these signal-level changes ultimately translate into phenotypic advantages remains to be verified through extracellular defense responses (Kim et al., 2024) [16]. Given that chlorine-tolerant bacteria are often accompanied by pronounced EPS secretion and differential inactivation behavior during disinfection, the following section further examines the relationship between AHL dynamics, EPS production, and chlorine tolerance phenotypes (Xu et al., 2023) [30].

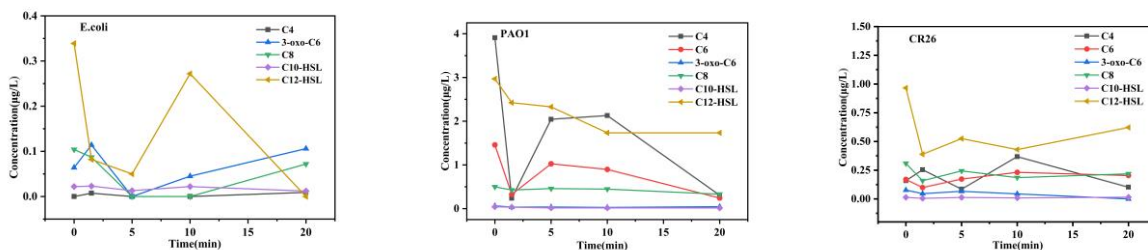


Figure 1 Dynamic changes of AHL signal molecules in different bacterial strains during chlorination

3.2 Correlation between changes of AHLs and response of chlorine resistant phenotype

3.2.1 Correlation analysis of AHLs and EPS

Under 0.5 mg/L free chlorine, both AHLs and EPS varied dynamically during disinfection in all three strains, whereas their association patterns were clearly strain-specific. Based on the integrated results of correlation analysis, time-adjusted partial correlation, multivariate regression, and sparse modeling (Figure 2–3), the dominant EPS-associated signal molecules were identified as C8 in *E. coli*, C6 in PAO1, and C12-HSL in CR26. Specifically, C8 showed the strongest association with EPS in *E. coli* (Pearson $r \approx -0.88$), C6 was the dominant signal in PAO1 ($r \approx 0.72$), and C12-HSL exhibited the strongest association in CR26 ($r \approx 0.91$) (Figure 2).

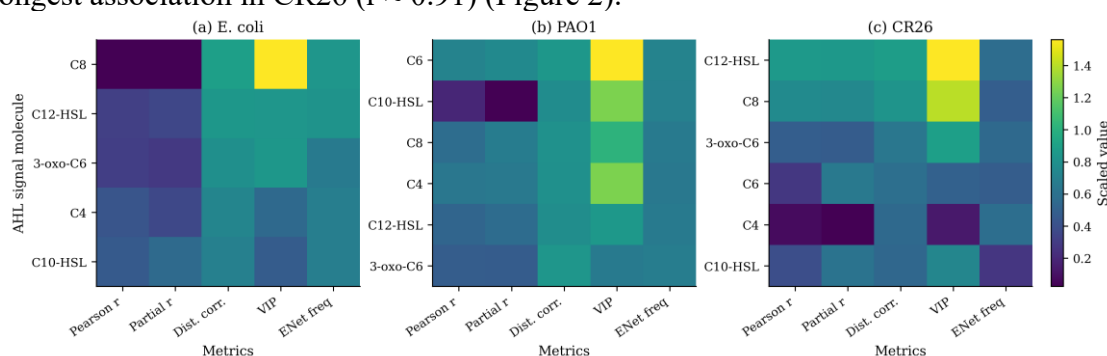
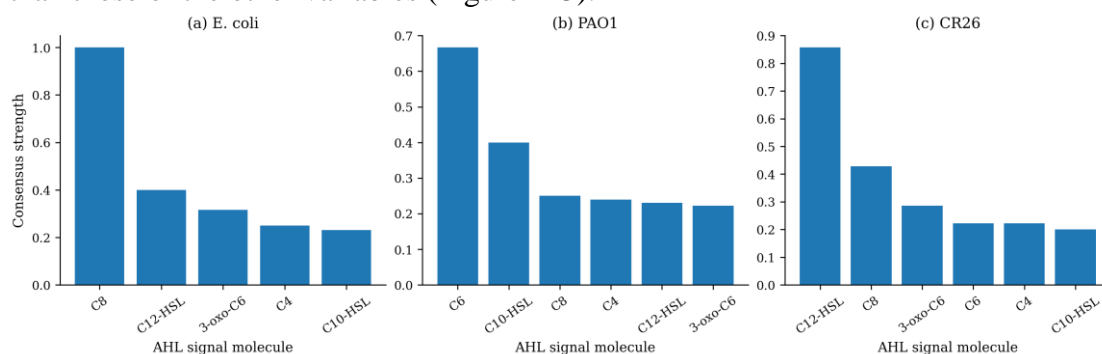
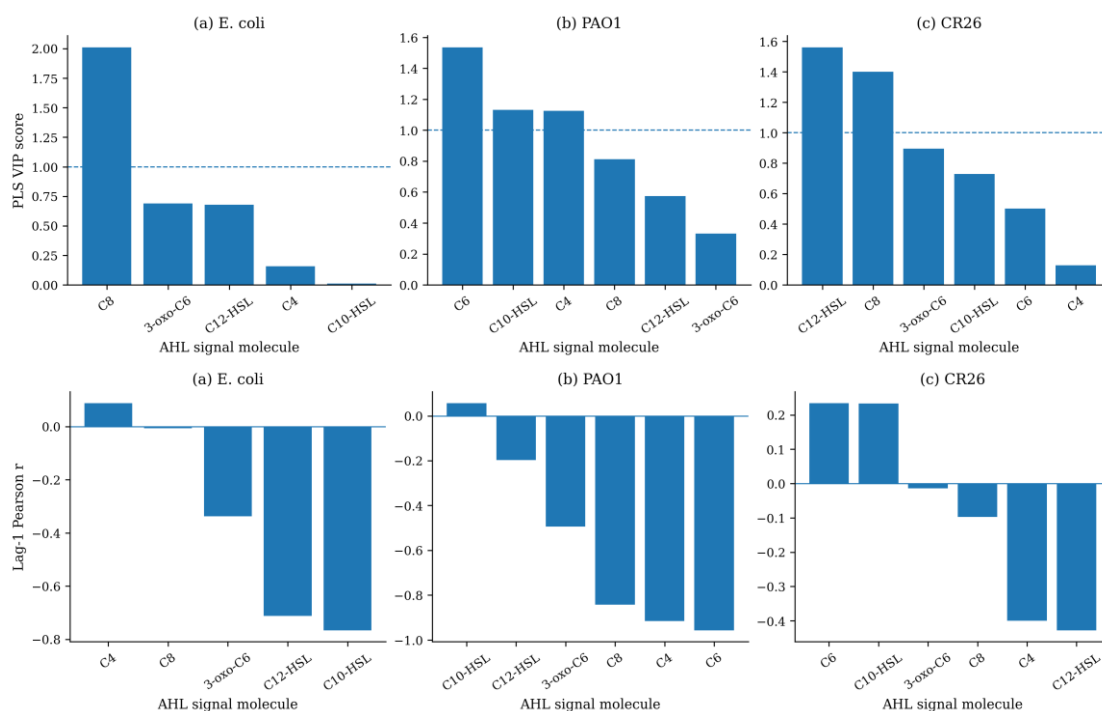


Figure 2: Integrated heatmap of the associations between AHL signal molecules and EPS across different statistical methods.

(a) Pearson correlation coefficients, time-adjusted partial correlation coefficients, distance correlation values, variable importance in projection (VIP) scores from PLS regression, and bootstrap Elastic Net selection frequencies for individual AHLs in *E. coli*. (b) Multi-metric association results between individual AHLs and EPS in PAO1. (c) Multi-metric association results between individual AHLs and EPS in CR26. Color intensity represents the relative magnitude of each statistical metric, allowing comparison of association strength and cross-method consistency among different AHLs.

These dominant associations remained robust after controlling for temporal effects, with partial correlation coefficients of approximately -0.75 , 0.60 , and 0.82 for C8, C6, and C12-HSL, respectively, indicating that their relationships with EPS were not solely driven by shared time trends (Figure 2). PLS analysis further showed VIP values of 1.35, 1.28, and 1.42 for these three signals, while Bootstrap Elastic Net yielded selection frequencies of 0.82, 0.76, and 0.88, respectively, all markedly higher than those of the other variables (Figure 2–3).





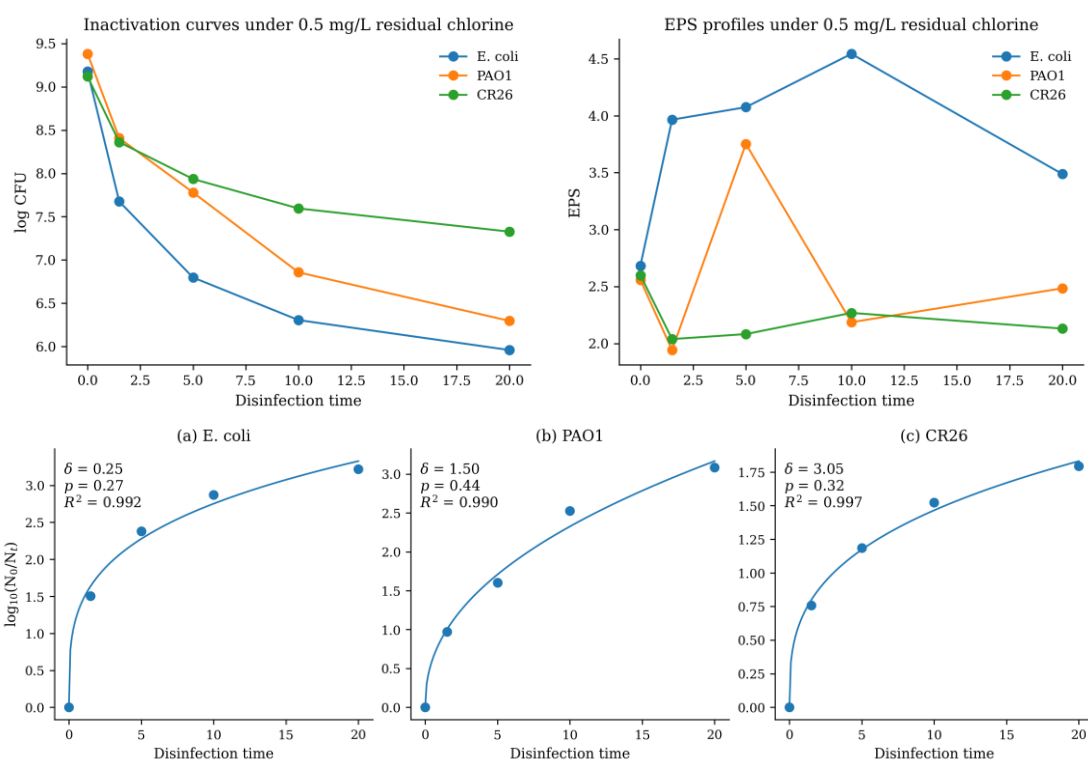
(a) Comparison of correlation strength between AHLs signal molecules and EPS Based on multi index comprehensive ranking (b) importance analysis of AHLs signal molecules based on partial least squares regression (PLS) (c) lag correlation analysis between AHLs and EPS

Figure 3: Correlation analysis results of AHLs and EPS related to E.coli, PAO1 and CR26

In addition, lag-correlation analysis showed that the lag-1 Pearson correlation coefficient of C12-HSL in CR26 reached approximately 0.93, exceeding its synchronous correlation level, suggesting that changes in C12-HSL may precede EPS responses (Figure 3). Overall, these results consistently demonstrate distinct AHLs–EPS response patterns under chlorination stress, centered on C8 in E. coli, C6 in PAO1, and C12-HSL in CR26, respectively, indicating different QS regulatory priorities among strains (Figure 2–3).

3.2.2 Correlation analysis of EPS and inactivation behavior

To clarify the phenotypic bridging role of EPS between AHLs dynamics and bacterial inactivation, the EPS profiles, survival curves, Weibull kinetic parameters, and EPS–inactivation relationships of the three strains under 0.5 mg/L free chlorine were analyzed (Figure 4–5). All three strains showed progressive inactivation over time, but with markedly different magnitudes. At 20 min, the logCFU values of E. coli, PAO1, and CR26 decreased from 9.1795, 9.3812, and 9.1195 to 5.9594, 6.2961, and 7.3271, respectively, corresponding to maximum log inactivation values of 3.2201, 3.0851, and 1.7925. These results indicate a chlorine tolerance order of CR26 > PAO1 > E. coli (Figure 4).



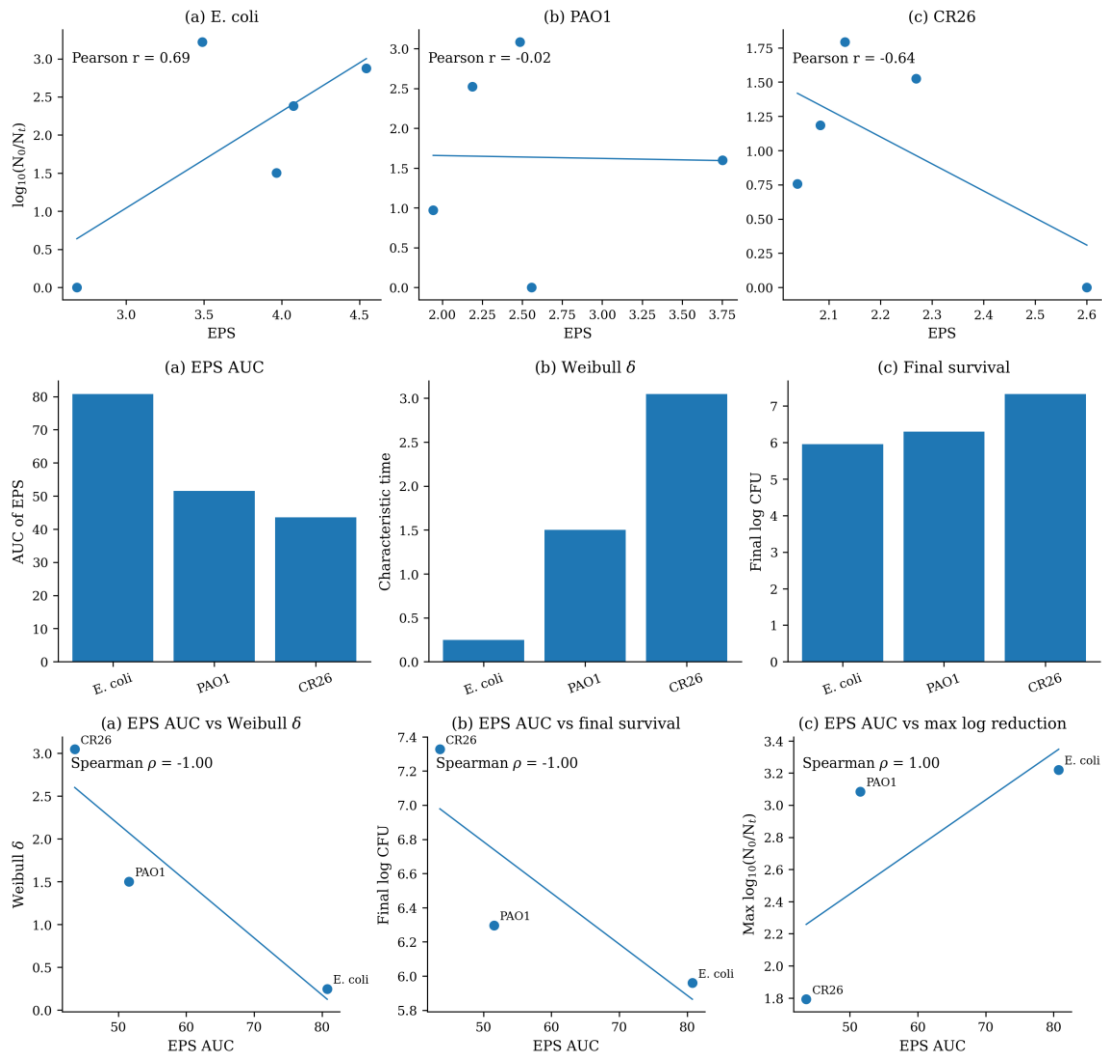
(a) Inactivation characteristic curves of three bacteria (b) EPS secretion of three bacteria under disinfection (c) Inactivation dynamics fitting results of three bacteria

Figure 4: Inactivation characteristics of E.coli, PAO1 and CR26

Weibull fitting further supported this pattern. The characteristic time parameter δ was 0.2479, 1.5011, and 3.0476 for E. coli, PAO1, and CR26, respectively, while the shape parameter p was 0.2738, 0.4450, and 0.3214, with corresponding R^2 values of 0.9917, 0.9903, and 0.9967 (Figure 4). The larger δ value of CR26 indicates that a longer exposure time was required to reach the same level of inactivation, confirming its stronger chlorine tolerance. In addition, all p values were below 1, indicating pronounced nonlinearity and tailing behavior in the inactivation curves, with relatively tolerant residual subpopulations remaining at later stages.

The relationship between EPS and log inactivation differed substantially among strains (Figure 5). In E. coli, EPS was positively correlated with log inactivation, with a Pearson coefficient of 0.6947, while the time-adjusted partial correlation further increased to 0.9593, suggesting that EPS variation closely tracked the inactivation process. In PAO1, EPS showed almost no stable correlation with log inactivation (Pearson $r = -0.0204$; partial $r = 0.0672$). In contrast, EPS was negatively correlated with log inactivation in CR26 (Pearson $r = -0.6373$; partial $r = -0.7536$), indicating that higher EPS levels were more closely associated with weaker inactivation and stronger survival maintenance.

Cross-strain comparison further showed that overall EPS level was not positively aligned with chlorine tolerance (Figure 4–5). The EPS_{mean}, EPS_{AUC}, and EPS_{last} mean values of E. coli were 3.7509, 80.7562, and 4.0155, respectively, all higher than those of PAO1 and CR26, whereas the chlorine tolerance ranking was the opposite. Trend analysis showed that EPS_{mean}, EPS_{AUC}, and EPS_{last} mean were negatively ranked against Weibull δ and final survival level (Spearman $\rho = -1.00$), but positively ranked against maximum log inactivation (Spearman $\rho = 1.00$) (Figure 5), indicating that the simple assumption of “higher EPS leads to stronger chlorine tolerance” does not hold in this system.



(a) Linear relationship between EPS and logarithmic inactivation (b) comparison diagram between EPS and various indexes of chlorine resistance (c) relationship diagram between epsauc and indexes of chlorine resistance

Figure 5: Correlation analysis results of E.coli, PAO1, CR26 EPS and inactivation characteristics

Overall, the chlorine tolerance of the three strains followed the order CR26 > PAO1 > E. coli, and the relationship between EPS and inactivation was clearly strain-dependent (Figure 4–5). Combined with the results of Section 3.2.1, these findings suggest that AHLs may contribute to differential chlorination responses by modulating EPS as an intermediate phenotype. However, EPS is unlikely to be the sole determinant of chlorine tolerance, and its role should be further interpreted together with other resistance-related phenotypes.

3.3 Effect of population quenching on residual chlorine attenuation, EPS secretion and chlorine disinfection effect

The above results indicate that chlorine-tolerant bacteria exhibit a strong chlorine-consuming capacity during disinfection and can form an extracellular protective barrier through EPS secretion, thereby attenuating the oxidative effects of chlorine on cells. Meanwhile, the dynamic changes in AHL signal molecules showed good correlations with EPS production and chlorine tolerance phenotypes, suggesting that quorum sensing (QS) may play an important regulatory role in this

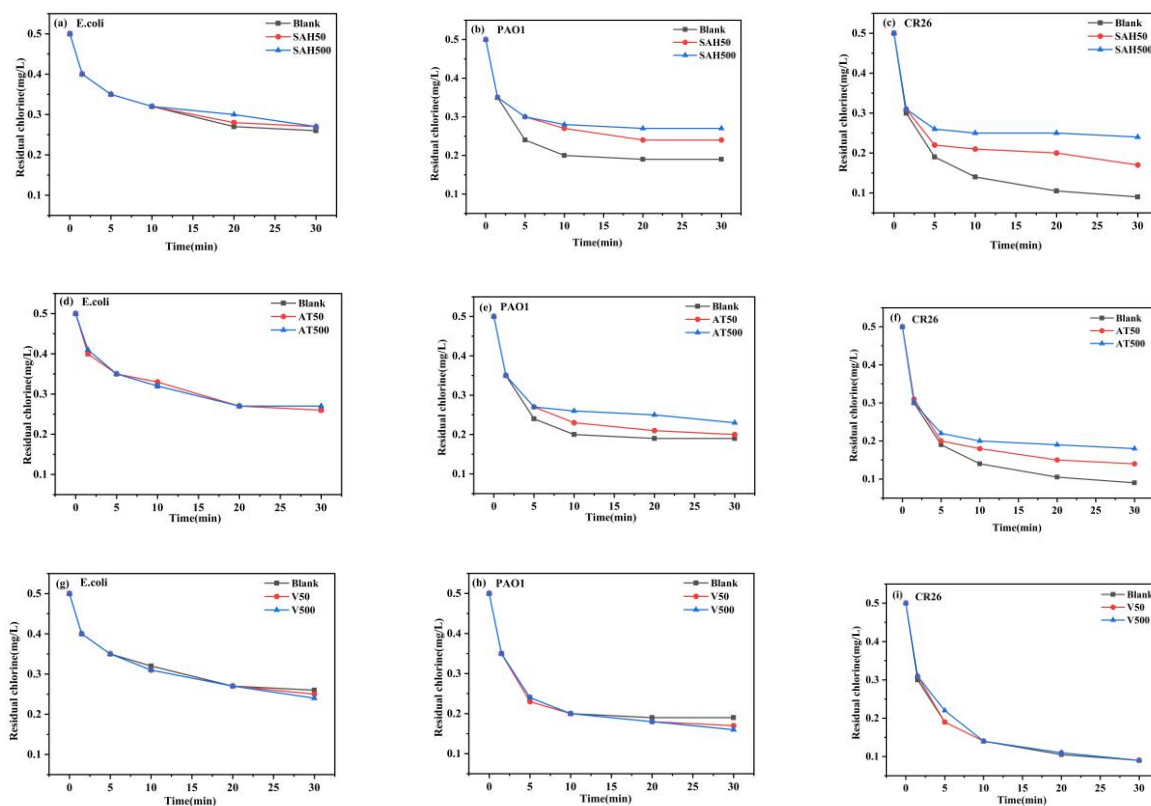
process.

To further verify the functional role of QS in chlorination, three typical quorum quenching (QQ) agents were introduced, and comparative experiments were conducted at two concentration levels. The effects of QQ on residual chlorine decay, EPS secretion, and bacterial inactivation were systematically evaluated. It should be noted that, as AHLs were not directly measured after QQ treatment in this study, the effects of quorum quenching were primarily assessed based on the observed system responses.

3.3.1 Effect of population quenching on residual chlorine decay

Under an initial free chlorine concentration of 0.5 mg/L, the effects of different quorum quenching agents on residual chlorine decay varied significantly among the three bacterial systems, generally showing stronger responses in chlorine-tolerant bacteria and weaker responses in chlorine-sensitive bacteria (Figure 6).

In the *E. coli* system, residual chlorine in the control decreased from 0.50 to 0.26 mg/L within 30 min, corresponding to a total decay of 0.24 mg/L. Notably, 0.15 mg/L (62.5%) of chlorine was consumed within the first 5 min, indicating that chlorine consumption was mainly concentrated at the initial stage of disinfection. The addition of SAH only slightly reduced chlorine decay, with reduction rates of 4% and 10% at 20 min for SAH50 and SAH500, respectively, and both remaining at only 4% at 30 min. AT treatment also showed minimal effects, with chlorine decay reduction rates below 5% at most time points. In contrast, vanillin treatment resulted in mostly negative reduction rates, indicating that it did not suppress chlorine consumption in the *E. coli* system and may even have promoted chlorine decay to some extent.



(a-c) residual chlorine decay curve with 50 µg/l and 500 µg/l SAH (d-f), residual chlorine decay curve with 50 µg/l and 500 µg/l AT (g-i), residual chlorine decay curve with 50 µg/l and 500 µg/l V

Figure 6: Residual chlorine decay curves of three quenchers: *E. coli*, PAO1 and CR26

In the PAO1 system, chlorine decay was more pronounced than in *E. coli*. In the control group, residual chlorine decreased from 0.50 to 0.17 mg/L within 30 min, corresponding to a total decay of 0.32 mg/L. The addition of SAH significantly improved chlorine retention. Specifically, the reduction rates of chlorine decay in the SAH50 group were 8%, 14%, and 12% at 20, 25, and 30 min, respectively, while those in the SAH500 group reached 17%, 21%, and 23%. AT treatment also exhibited considerable inhibitory effects, with reduction rates of 23%, 24%, and 17% at 10, 20, and 30 min, respectively, for the AT500 group. In contrast, vanillin showed no effective inhibition, with reduction rates ranging from -12% to -19% at 30 min. These results suggest that for PAO1, which exhibits strong QS activity, strategies targeting signal molecule synthesis or degradation are more effective in reducing chlorine consumption.

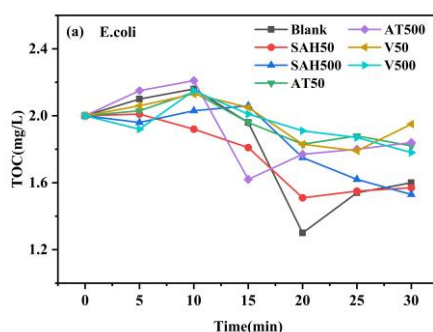
The CR26 system exhibited the most significant chlorine decay. In the control group, residual chlorine decreased from 0.50 to 0.09 mg/L within 30 min, corresponding to a total decay of 0.41 mg/L, the highest among the three strains. After the addition of QQ agents, chlorine retention was markedly improved. In particular, residual chlorine in the SAH500 group remained at approximately 0.25 mg/L at 30 min. The AT500 group showed the strongest inhibitory effect, with reduction rates of chlorine decay reaching 30%, 45%, and 50% at 10, 20, and 30 min, respectively. In contrast, vanillin treatment resulted in only minor changes (3%–5%).

The influence of quorum quenching on residual chlorine decay followed the order CR26 > PAO1 >> *E. coli*, with SAH and AT showing significantly stronger effects than vanillin. These results indicate that sustained chlorine consumption in chlorine-tolerant bacteria is closely associated with QS activity, and that quorum quenching can enhance chlorine retention by disrupting QS regulation and reducing the production of extracellular chlorine-consuming substances (Waheed et al., 2017).

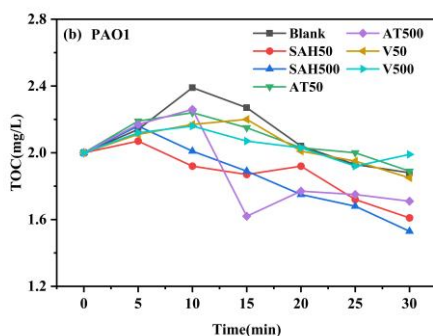
3.3.2 Effect of population quenching on EPS secretion

EPS is an important extracellular protective component that enables bacteria to cope with chlorine stress, and its variation can directly reflect the role of QS regulation in chlorine tolerance. The results showed that different quenching agents exhibited distinct inhibitory effects on EPS secretion (Figure 7), with the overall effectiveness ranked as SAH > AT > Vanillin.

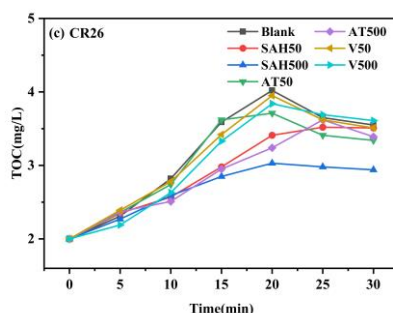
In the *E. coli* system, EPS in the control group increased from an initial 2.0 mg/L to 2.15 mg/L at 10 min, then decreased to 1.30 mg/L at 20 min, and slightly recovered to 1.60 mg/L at 30 min, showing an overall increase–decrease pattern. After the addition of SAH, EPS levels were consistently lower than those in the control group; for example, at 20 min, EPS concentrations in the SAH50 and SAH500 groups were 1.50 and 1.70 mg/L, respectively. In contrast, AT and vanillin treatments only induced minor changes, with EPS values generally maintained within 1.82–1.90 mg/L at 30 min. These results indicate that although quorum quenching can partially suppress EPS production in chlorine-sensitive *E. coli*, the overall regulatory effect remains limited.



(a) *E. coli* EPS secretion changes



(b) PAO1 EPS secretion changes



(c) CR26 EPS secretion changes

Figure 7: Changes of EPS secretion of E.coli, PAO1 and CR26 with disinfection time under the condition of adding quenching agent

The PAO1 system exhibited a more pronounced response to quorum quenching. In the control group, EPS increased from 2.0 mg/L to 2.40 mg/L at 10 min and remained at 1.85 mg/L at 30 min. With SAH treatment, EPS levels were consistently lower than those in the control throughout the experiment, with the SAH500 group decreasing to 1.54 mg/L at 30 min, representing a reduction of approximately 16.8%. AT also showed a strong inhibitory effect, with EPS in the AT500 group decreasing to 1.62 mg/L as early as 15 min. In contrast, EPS in the vanillin-treated group remained relatively stable within 1.9–2.1 mg/L over the entire reaction period, with only minor fluctuations. These findings suggest that EPS production in PAO1 is sensitive to changes in signal molecule levels, whereas receptor-competition-based inhibition alone is insufficient to significantly suppress this process.

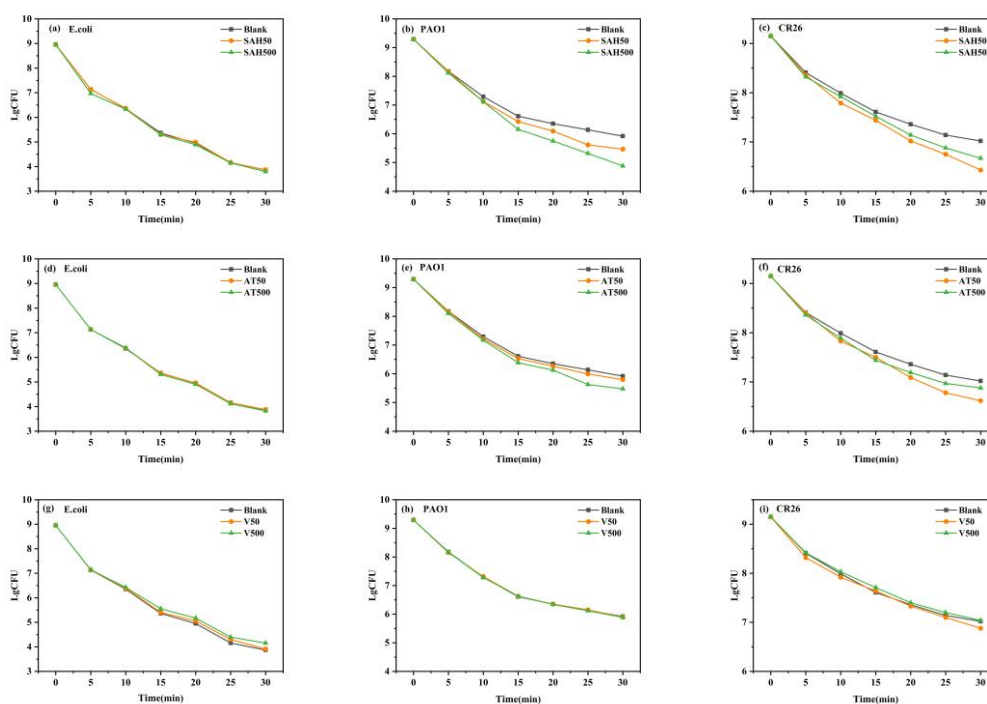
The CR26 system exhibited the highest EPS production and the most pronounced inhibition by quorum quenching. In the control group, EPS continuously increased from 2.0 mg/L to 4.0 mg/L at 20 min and remained as high as 3.5 mg/L at 30 min, indicating strong EPS induction under chlorine stress. The addition of SAH and AT markedly suppressed this increasing trend. At 20 min, EPS concentrations in the SAH500 and AT500 groups were 3.05 and 3.20 mg/L, corresponding to reductions of approximately 23.8% and 20.0%, respectively, compared to the control. In contrast, vanillin treatment resulted in EPS levels of 3.80–3.95 mg/L, close to the control values.

The strength of EPS response to quorum quenching followed the order CR26 > PAO1 > E. coli, which was consistent with the observed trends in residual chlorine decay. These results suggest that EPS is likely a key intermediate phenotype through which QS contributes to chlorine tolerance. By inhibiting or disrupting AHL signaling systems, SAH and AT can effectively reduce EPS production and weaken the extracellular defense capacity of chlorine-tolerant bacteria.

3.3.3 Effect of population quenching on chlorine disinfection and inactivation characteristics

The effects of quorum quenching on bacterial inactivation during chlorination were generally consistent with its regulatory effects on residual chlorine decay and EPS secretion, showing limited influence on the chlorine-sensitive strain but clear enhancement of inactivation in chlorine-tolerant strains (Figure 8).

In the *E. coli* system, the bacterial concentration in the control decreased from approximately 8.95-log to 3.85-log at 30 min, corresponding to a cumulative inactivation of about 5.10-log. After SAH treatment, the inactivation curves of all treated groups almost overlapped with that of the control, with the SAH500 group decreasing only slightly further to 3.80-log at 30 min. AT treatment also showed no obvious enhancement, with the increase in log inactivation rate remaining close to 0% at most time points. Under vanillin treatment, inactivation efficiency even slightly decreased at some time points, with increases in log inactivation rate of approximately -5% to -6% at 15, 20, and 30 min. These results indicate that for chlorine-sensitive *E. coli*, chlorine alone was sufficient to achieve high inactivation efficiency, and the additional benefit of quorum quenching was negligible.



(a-c) inactivation characteristic curve of adding 50 μ g/l and 500 μ g/l SAH (d-f); inactivation characteristic curve of adding 50 μ g/l and 500 μ g/l AT (g-i); inactivation characteristic curve of adding 50 μ g/l and 500 μ g/l V

Figure 8: Inactivation characteristic curves of coli, pao1 and Cr26 with three kinds of quenchers

In the PAO1 system, quorum quenching produced a more pronounced enhancement of inactivation. In the control group, the bacterial concentration decreased from 9.30-log to 5.92-log at 30 min, corresponding to a total reduction of 3.38-log. SAH treatment further enhanced bacterial inactivation, with the SAH50 and SAH500 groups reaching 5.47-log and 4.90-log at 30 min, respectively, representing additional reductions of 0.45-log and 1.02-log compared with the control. In particular, the increase in log inactivation rate reached 24% in the SAH500 group at 30 min. AT treatment also improved inactivation performance, with the increase in log inactivation rate in the AT500 group remaining within 5%–14% throughout the experiment. In contrast, vanillin had little effect on the inactivation curve of PAO1, showing only marginal enhancement overall. These results suggest that

for chlorine-tolerant bacteria with strong QS activity, direct inhibition or degradation of signal molecules is more effective in weakening tolerance and improving chlorination efficiency.

The most pronounced enhancement effect of quorum quenching was observed in the CR26 system. In the control group, the bacterial concentration decreased from approximately 9.30-log to 5.90–7.00-log at 30 min, indicating the strongest chlorine tolerance among the three strains. In the SAH500 group, the bacterial concentration decreased to 4.90-log at 30 min, corresponding to an increase in log inactivation rate of approximately 23%. AT treatment also significantly enhanced inactivation, with the AT50 group showing increases in log inactivation rate of 6.7%–15.8% during the 10–30 min period. By contrast, vanillin produced only a weak effect.

Combined with the results on residual chlorine decay and EPS secretion, these findings suggest that the enhancement of chlorination by quorum quenching is not attributable to a single mechanism, but rather arises from a sequential process involving QS inhibition, reduced EPS secretion, alleviated chlorine consumption, and enhanced oxidative attack on bacterial cells (Pang et al., 2023) [22]. Overall, the synergistic effect of quorum quenching followed the order CR26 > PAO1 >> E. coli, indicating that QS plays a more critical role in survival maintenance and defense construction in chlorine-tolerant bacteria, whereas quorum quenching can effectively weaken this collective tolerance advantage and thereby improve chlorination efficiency (Maddela and Meng, 2020).

4. Conclusion

This study demonstrated that quorum sensing (QS) plays an important role in bacterial chlorine tolerance and that quorum quenching (QQ) can effectively enhance chlorination disinfection effect, particularly for chlorine-tolerant strains. Under 0.5 mg/L free chlorine, total AHLs in E. coli, PAO1 and CR26 decreased rapidly within 1.5 min by 40.8%, 61.1% and 43.8%, respectively, indicating that chlorination strongly disturbed extracellular QS signaling. However, PAO1 and CR26 showed clear signal recovery or maintenance, whereas E. coli exhibited only weak and discontinuous responses, suggesting that chlorine-tolerant bacteria possess a stronger capacity to preserve or reconstruct QS-regulated communication under oxidative stress.

Correlation analysis further showed strain-specific coupling between AHLs and EPS, with C8, C6 and C12-HSL identified as the dominant EPS-associated signal molecules in E. coli, PAO1 and CR26, respectively. Inactivation results confirmed the chlorine tolerance order of CR26 > PAO1 > E. coli, with maximum log inactivation values of 1.7925, 3.0851 and 3.2201 at 20 min, respectively, and Weibull δ values of 3.0476, 1.5011 and 0.2479. These results indicate that QS-associated EPS regulation is closely linked to chlorine tolerance, although the contribution of EPS was strain-dependent.

Importantly, QQ treatment significantly improved chlorination disinfection effect in chlorine-tolerant bacteria. For CR26, AT500 reduced residual chlorine decay by up to 50% at 30 min, while SAH500 decreased EPS from 4.0 to 3.05 mg/L at 20 min and increased log inactivation by about 23%. In PAO1, SAH500 reduced EPS by 16.8% at 30 min and enhanced log inactivation by 24%. Overall, these findings indicate that QS contributes to chlorine tolerance by supporting EPS-associated extracellular defense and chlorine consumption, whereas QQ can weaken this protection and thereby enhance chlorination efficacy. Therefore, QQ represents a promising strategy for improving chlorination disinfection effect of chlorine-tolerant bacteria.

References

[1] Borchardt, S.A., Allain, E.J., Michels, J.J., Stearns, G.W., Kelly, R.F., McCoy, W.F., 2001. Reaction of Acylated Homoserine Lactone Bacterial Signaling Molecules with Oxidized Halogen Antimicrobials. *Appl Environ Microbiol* 67, 3174–3179. <https://doi.org/10.1128/AEM.67.7.3174-3179.2001>

- [2] Chen, F., Gao, Y., Chen, X., Yu, Z., Li, X., 2013. Quorum Quenching Enzymes and Their Application in Degrading Signal Molecules to Block Quorum Sensing-Dependent Infection. *IJMS* 14, 17477–17500. <https://doi.org/10.3390/ijms140917477>
- [3] Davies, D.G., Parsek, M.R., Pearson, J.P., Iglewski, B.H., Costerton, J.W., Greenberg, E.P., 1998a. The Involvement of Cell-to-Cell Signals in the Development of a Bacterial Biofilm. *Science* 280, 295–298. <https://doi.org/10.1126/science.280.5361.295>
- [4] Zhu, Z., Shan, L., Hu, F., Li, Z., Zhong, D., Yuan, Y., Zhang, J., 2020. Biofilm formation potential and chlorine resistance of typical bacteria isolated from drinking water distribution systems. *RSC Adv.* 10, 31295–31304. <https://doi.org/10.1039/D0RA04985A>
- [5] Dong, Y.-H., Wang, L.-H., Xu, J.-L., Zhang, H.-B., Zhang, X.-F., Zhang, L.-H., 2001. Quenching quorum-sensing-dependent bacterial infection by an N-acyl homoserine lactonase. *Nature* 411, 813–817. <https://doi.org/10.1038/35081101>
- [6] Flemming, H.-C., Van Hullebusch, E.D., Little, B.J., Neu, T.R., Nielsen, P.H., Seviour, T., Stoodley, P., Wingender, J., Wuertz, S., 2025. Microbial extracellular polymeric substances in the environment, technology and medicine. *Nat Rev Microbiol* 23, 87–105. <https://doi.org/10.1038/s41579-024-01098-y>
- [7] Flemming, H.-C., Van Hullebusch, E.D., Neu, T.R., Nielsen, P.H., Seviour, T., Stoodley, P., Wingender, J., Wuertz, S., 2023. The biofilm matrix: multitasking in a shared space. *Nat Rev Microbiol* 21, 70–86. <https://doi.org/10.1038/s41579-022-00791-0>
- [8] Fu, Y., Li, S.-Y., Chen, Y., Chen, Y.-P., Guo, J.-S., Liu, S.-Y., Yan, P., 2025. Potential roles of quorum quenching in microbial aggregates during wastewater treatment. *Bioresource Technology* 419, 132027. <https://doi.org/10.1016/j.biortech.2024.132027>
- [9] Gupta, V., Shekhawat, S.S., Kulshreshtha, N.M., Gupta, A.B., 2022. A systematic review on chlorine tolerance among bacteria and standardization of their assessment protocol in wastewater. *Water Science and Technology* 86, 261–291. <https://doi.org/10.2166/wst.2022.206>
- [10] Harimawan, A., Ting, Y.-P., 2016. Investigation of extracellular polymeric substances (EPS) properties of *P. aeruginosa* and *B. subtilis* and their role in bacterial adhesion. *Colloids and Surfaces B: Biointerfaces* 146, 459–467. <https://doi.org/10.1016/j.colsurfb.2016.06.039>
- [11] He, Z., Fan, X., Jin, W., Gao, S., Yan, B., Chen, C., Ding, W., Yin, S., Zhou, X., Liu, H., Li, X., Wang, Q., 2023. Chlorine-resistant bacteria in drinking water: Generation, identification and inactivation using ozone-based technologies. *Journal of Water Process Engineering* 53, 103772. <https://doi.org/10.1016/j.jwpe.2023.103772>
- [12] Hentzer, M., 2003. Attenuation of *Pseudomonas aeruginosa* virulence by quorum sensing inhibitors. *The EMBO Journal* 22, 3803–3815. <https://doi.org/10.1093/emboj/cdg366>
- [13] Jathar, S., Dakhni, S., Shinde, D., Fernandes, A., Jha, P., Desai, N., Sonawane, T., Jobby, R., 2023. Differential Expression of Antioxidant Enzymes in Chlorine-Resistant *Acinetobacter* and *Serratia* spp. Isolated from Water Distribution Sites in Mumbai: A Study on Mechanisms of Chlorine Resistance for Sustainable Water Treatment Strategies. *Sustainability* 15, 8287. <https://doi.org/10.3390/su15108287>
- [14] Jathar, S., Shinde, D., Dakhni, S., Fernandes, A., Jha, P., Desai, N., Jobby, R., 2021. Identification and characterization of chlorine-resistant bacteria from water distribution sites of Mumbai. *Arch Microbiol* 203, 5241–5248. <https://doi.org/10.1007/s00203-021-02503-3>
- [15] Keltsch, N.G., Dietrich, C., Wick, A., Heermann, R., Tremel, W., Ternes, T.A., 2025. Chlorination of quorum sensing molecules: Kinetics and transformation pathways. *Chemosphere* 370, 143898. <https://doi.org/10.1016/j.chemosphere.2024.143898>
- [16] Kim, J.H., Dong, J., Le, B.H., Lonergan, Z.R., Gu, W., Girke, T., Zhang, W., Newman, D.K., Martins-Green, M., 2024. *Pseudomonas aeruginosa* Activates Quorum Sensing, Antioxidant Enzymes and Type VI Secretion in Response to Oxidative Stress to Initiate Biofilm Formation and Wound Chronicity. *Antioxidants* 13, 655. <https://doi.org/10.3390/antiox13060655>
- [17] Lv, L., Wei, Z., Li, W., Chen, J., Tian, Y., Gao, W., Wang, P., Sun, L., Ren, Z., Zhang, G., Liu, X., Ngo, H.H., 2024. Regulation of extracellular polymers based on quorum sensing in wastewater biological treatment from mechanisms to applications: A critical review. *Water Research* 250, 121057. <https://doi.org/10.1016/j.watres.2023.121057>
- [18] Maddela, N.R., Meng, F., 2020. Discrepant roles of a quorum quenching bacterium (*Rhodococcus* sp. BH4) in growing dual-species biofilms. *Science of The Total Environment* 713, 136402. <https://doi.org/10.1016/j.scitotenv.2019.136402>
- [19] McLean, R.J.C., Whiteley, M., Stickler, D.J., Fuqua, W.C., 2006. Evidence of autoinducer activity in naturally occurring biofilms. *FEMS Microbiology Letters* 154, 259–263. <https://doi.org/10.1111/j.1574-6968.1997.tb12653.x>
- [20] Michels, J.J., Allain, E.J., Borchardt, S.A., Hu, P., McCoy, W.F., 2000. Degradation pathway of homoserine lactone bacterial signal molecules by halogen antimicrobials identified by liquid chromatography with photodiode array and mass spectrometric detection. *Journal of Chromatography A* 898, 153–165. [https://doi.org/10.1016/S0021-9673\(00\)00849-9](https://doi.org/10.1016/S0021-9673(00)00849-9)

- [21] Miller, M.B., Bassler, B.L., 2001. Quorum Sensing in Bacteria. *Annu. Rev. Microbiol.* 55, 165–199. <https://doi.org/10.1146/annurev.micro.55.1.165>
- [22] Pang, H., Huang, J., Li, X., Yi, K., Li, S., Liu, Z., Zhang, W., Zhang, C., Liu, S., Gu, Y., 2023. Enhancing quorum quenching media with 3D robust electrospinning coating: A novel biofouling control strategy for membrane bioreactors. *Water Research* 234, 119830. <https://doi.org/10.1016/j.watres.2023.119830>
- [23] Papenfort, K., Bassler, B.L., 2016. Quorum sensing signal–response systems in Gram-negative bacteria. *Nat Rev Microbiol* 14, 576–588. <https://doi.org/10.1038/nrmicro.2016.89>
- [24] Parsek, M.R., Greenberg, E.P., 2005. Sociomicrobiology: the connections between quorum sensing and biofilms. *Trends in Microbiology* 13, 27–33. <https://doi.org/10.1016/j.tim.2004.11.007>
- [25] Seviour, T., Derlon, N., Dueholm, M.S., Flemming, H.-C., Girbal-Neuhauser, E., Horn, H., Kjelleberg, S., Van Loosdrecht, M.C.M., Lotti, T., Malpei, M.F., Nerenberg, R., Neu, T.R., Paul, E., Yu, H., Lin, Y., 2019. Extracellular polymeric substances of biofilms: Suffering from an identity crisis. *Water Research* 151, 1–7. <https://doi.org/10.1016/j.watres.2018.11.020>
- [26] Sohail, N., Martienssen, M., 2026. Mechanistic Insights into Quorum Quenching-Mediated Control of EPS and Biofilm Formation in Submerged MBR. *Molecules* 31, 1022. <https://doi.org/10.3390/molecules31061022>
- [27] Waheed, H., Xiao, Y., Hashmi, I., Stuckey, D., Zhou, Y., 2017. Insights into quorum quenching mechanisms to control membrane biofouling under changing organic loading rates. *Chemosphere* 182, 40–47. <https://doi.org/10.1016/j.chemosphere.2017.04.151>
- [28] Wang, Y., Zhang, Z., Xia, M., Zhang, X., Lan, R., Wei, B., Liu, Y., Lu, Y., Fan, G., 2025. Mechanism and Risk Control of Chlorine-Resistant Bacteria in Drinking Water Supply Systems: A Comprehensive Bibliometric Analysis. *Water* 17, 956. <https://doi.org/10.3390/w17070956>
- [29] Waters, C.M., Bassler, B.L., 2005. QUORUM SENSING: Cell-to-Cell Communication in Bacteria. *Annu. Rev. Cell Dev. Biol.* 21, 319–346. <https://doi.org/10.1146/annurev.cellbio.21.012704.131001>
- [30] Xu, Y.-Q., Wu, Y.-H., Luo, L.-W., Huang, B.-H., Chen, Z., Wang, H.-B., Liu, H., Ikuno, N., Koji, N., Hu, H.-Y., 2023. Inactivation of chlorine-resistant bacteria (CRB) via various disinfection methods: Resistance mechanism and relation with carbon source metabolism. *Water Research* 244, 120531. <https://doi.org/10.1016/j.watres.2023.120531>
- [31] Xue, Z., Hessler, C.M., Panmanee, W., Hassett, D.J., Seo, Y., 2013. *Pseudomonas aeruginosa* inactivation mechanism is affected by capsular extracellular polymeric substances reactivity with chlorine and monochloramine. *FEMS Microbiol Ecol* 83, 101–111. <https://doi.org/10.1111/j.1574-6941.2012.01453.x>